

Supplementary Materials: Routine Processing and Automatic Detection of Volcanic Ground Deformation using Sentinel-1 InSAR Data: Insights from African Volcanoes

Contents of this file

1. Tables S1 to S3
2. Figures S1 to S5

Table S1. List of the 30 volcanoes processed in the Afar region. For each of them, we indicate the latitude, the longitude, the mean coherence, the phase-elevation correlation and the velocity uncertainty due to the selection of the reference point.

Volcano Name	Lat °	Lon °	Mean Coherence	Topo correlation cdf($R^2=0.5$)	Velocity uncertainty (cm/yr)
Adwa	10.07	40.84	0.37	0.88	0.21
Alayta	12.89	40.57	0.78	0.84	0.59
Ale Bagu	13.51	40.63	0.72	0.96	0.57
Alid	14.88	39.92	0.63	0.59	1.02
Alu-Dalafilla	13.79	40.55	0.71	0.96	0.53
Ardoukoba	11.58	42.47	0.59	0.90	0.57
Asavyo	13.10	41.60	0.64	0.66	0.44
Assab	12.95	42.43	0.80	0.83	0.84
Ayelu	10.08	40.70	0.34	0.89	0.26
Bora Ale	13.73	40.60	0.73	0.95	0.56
Borawli	13.30	40.99	0.74	0.97	0.61
Dabbahu	12.60	40.48	0.60	0.96	0.84
Dabbayra	12.38	40.07	0.44	0.69	0.23
Dalol	14.24	40.30	0.54	0.82	0.40
Dama Ali	11.28	41.63	0.55	0.92	0.46
Dubbi	13.58	41.81	0.67	0.65	0.70
Erta Ale	13.60	40.67	0.75	0.98	0.40
Gabillema	11.08	41.27	0.67	0.94	0.39
Gada Ale	13.98	40.41	0.56	0.97	0.46
Groppi	11.82	40.24	0.35	0.99	0.18
Gufa	12.55	42.53	0.84	0.83	1.65
Hayli Gubbi	13.51	40.72	0.73	0.98	0.59
Ma Alalta	13.01	40.19	0.57	0.57	0.24
Manda Gargori	11.75	41.48	0.38	0.64	0.31
Manda-Inakir	12.38	42.20	0.57	0.88	0.32
Mat Ala	13.11	41.16	0.70	0.99	0.59
Mousa Alli	12.47	42.40	0.67	0.95	0.33
Nabro	13.37	41.70	0.63	0.79	0.78
Tat Ali	13.28	41.06	0.70	0.97	0.41
Yangudi	10.58	41.04	0.32	0.92	0.33

Table S2. List of the 16 volcanoes processed in the Main Ethiopian Rift. For each of them, we indicate the latitude, the longitude, the mean coherence, the phase-elevation correlation and the velocity uncertainty due to the selection of the reference point.

Volcano Name	Lat °	Lon °	Mean Coherence	Topo correlation cdf($R^2=0.5$)	Velocity uncertainty (cm/yr)
Alutu	7.77	38.78	0.17	0.92	0.59
Beru	8.95	39.75	0.30	0.83	0.42
Bishoftu	8.78	38.98	0.20	0.75	0.36
Bora-Bericha	8.22	39.05	0.16	0.89	0.37
Boset-Bericha	8.56	39.48	0.25	0.83	0.45
Butajiri-Silti Field	8.05	38.35	0.12	0.60	0.40
Corbettii	7.19	38.39	0.12	0.97	0.43
Dofan	9.35	40.13	0.26	0.84	0.27
East Zway	7.87	38.90	0.16	0.90	0.57
Fentale	8.98	39.93	0.29	0.90	0.34
Gedamsa	8.36	39.19	0.21	0.85	0.58
Hertali	9.78	40.33	0.29	0.98	0.36
Kone	8.79	39.70	0.30	0.89	0.35
O'a Caldera	7.47	38.58	0.15	0.98	0.67
Sodore	8.43	39.35	0.23	0.86	0.60
Tullu Moje	8.16	39.14	0.17	0.60	0.48

Table S3. List of the 17 volcanoes processed in the Kenya-Tanzania rift. For each of them, we indicate the latitude, the longitude, the mean coherence, the phase-elevation correlation and the velocity uncertainty due to the selection of the reference point.

Volcano Name	Lat °	Lon °	Mean Coherence	Topo correlation cdf($R^2=0.5$)	Velocity uncertainty (cm/yr)
Barrier	2.32	36.57	0.53	0.90	1.63
Chyulu Hills	-2.68	37.88	0.24	0.88	0.44
Ol Doinyo Eburru	-0.65	36.22	0.15	0.97	0.71
Elmenteita Badlands	-0.52	36.27	0.16	0.93	0.39
Emuruangogolak	1.50	36.33	0.50	0.77	0.40
Korosi	0.77	36.12	0.19	0.78	0.36
Ol Doinyo Lengai	-2.76	35.91	0.27	0.78	0.31
Longonot	-0.91	36.45	0.12	0.89	0.65
Menengai	-0.20	36.07	0.15	0.96	0.67
Meru	-3.25	36.75	0.20	0.97	0.37
Namarunu	1.98	36.43	0.56	0.85	0.75
Ol Kokwe	0.62	36.08	0.10	0.93	0.67
Olkaria	-0.90	36.29	0.13	0.97	0.54
Paka	0.92	36.18	0.21	0.77	0.35
Silali	1.15	36.23	0.29	0.76	0.31
South Island	2.63	36.60	0.42	0.97	1.56
Suswa	-1.15	36.36	0.24	0.91	0.56

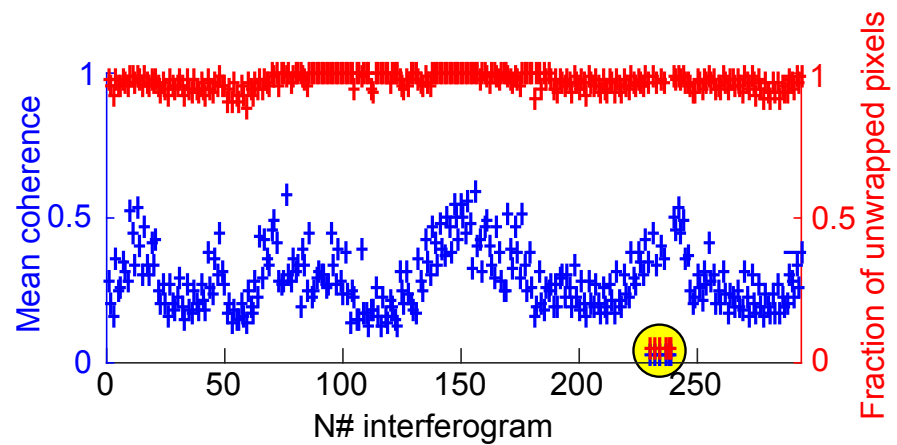


Figure S1. Quality check of LiCSAR products over Fentale volcano. For each interferogram, we plot the mean coherence (blue crosses) and the fraction of unwrapped pixels (red crosses). Among the 294 interferograms processed, six of them have values much lower than the common trend (yellow circles).

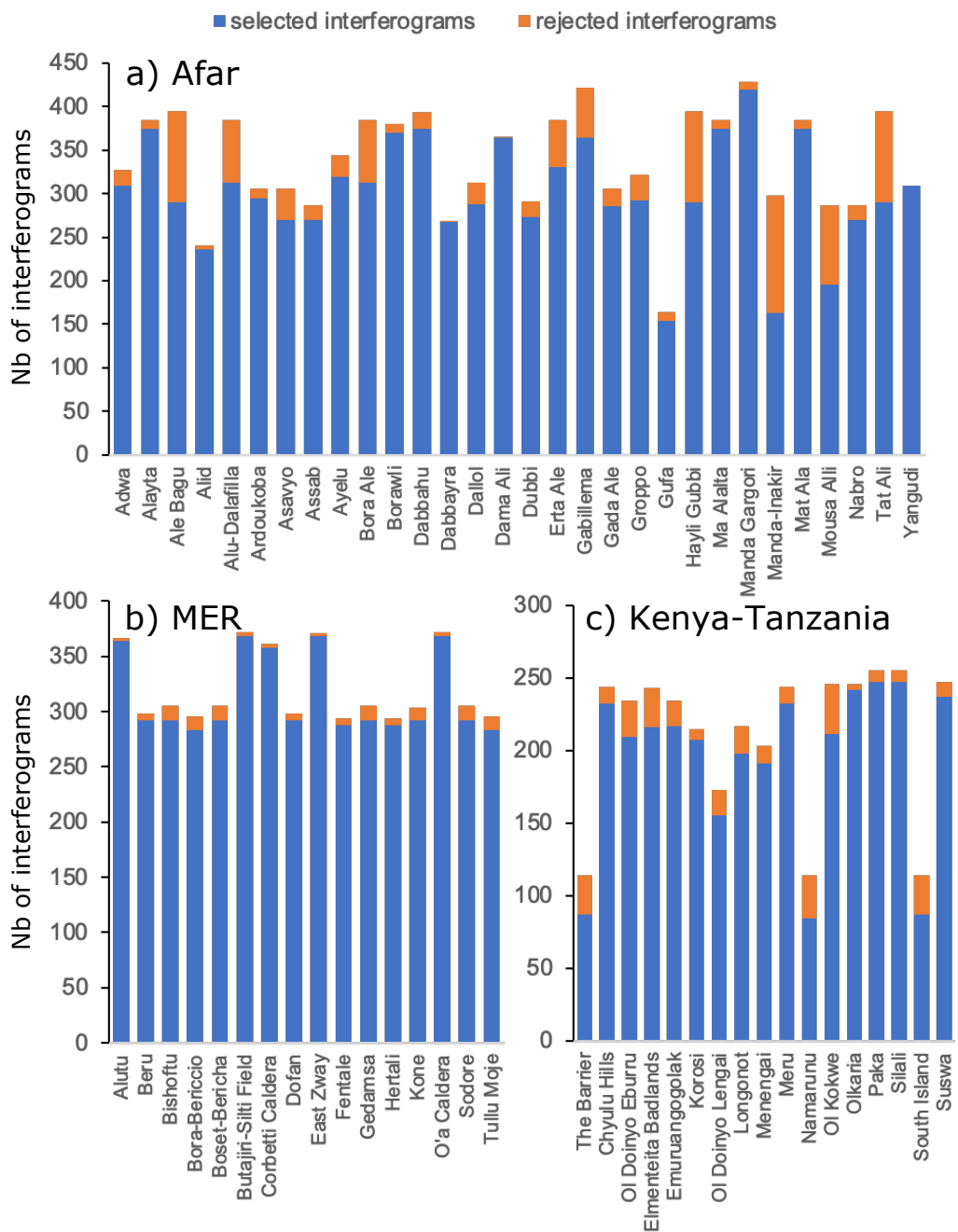


Figure S2. Number of interferograms processed per volcano for the three regions: a) Afar, b) MER and c) Kenya-Tanzania. Blue and red bars indicate the proportion of interferograms selected and rejected, respectively. The selection is based on the two criteria, mean coherence and fraction of unwrapped pixels, as described in Figure S1.

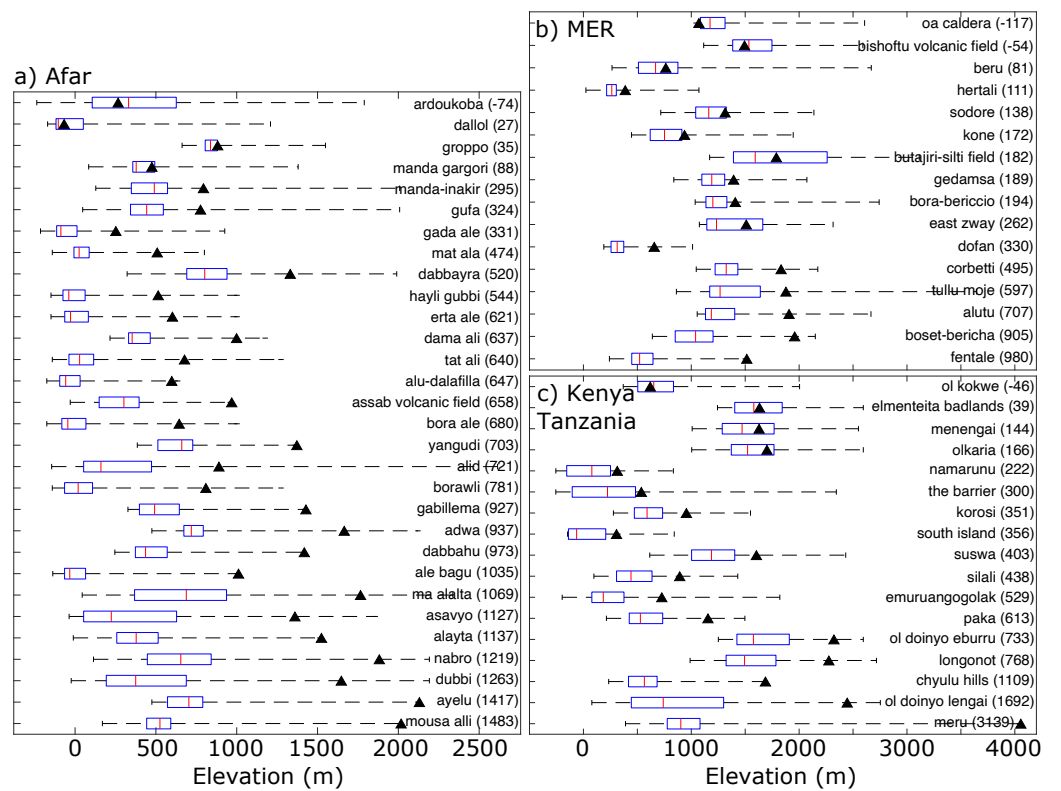


Figure S3. Boxplots of the elevation for each volcanic area processed ($0.5^\circ \times 0.5^\circ$) for a) Afar, b) MER and c)Kenya-Tanzania. Dashed lines show the range of elevation (between the minimum and maximum values) and blue rectangles indicate the interquartile range (between 25th and 75th percentiles). Red vertical lines correspond to the median elevation and black triangles indicate the maximum elevation of the volcanic edifice. Numbers in brackets indicate the volcano's height evaluated as the difference between the median value and the edifice's elevation.

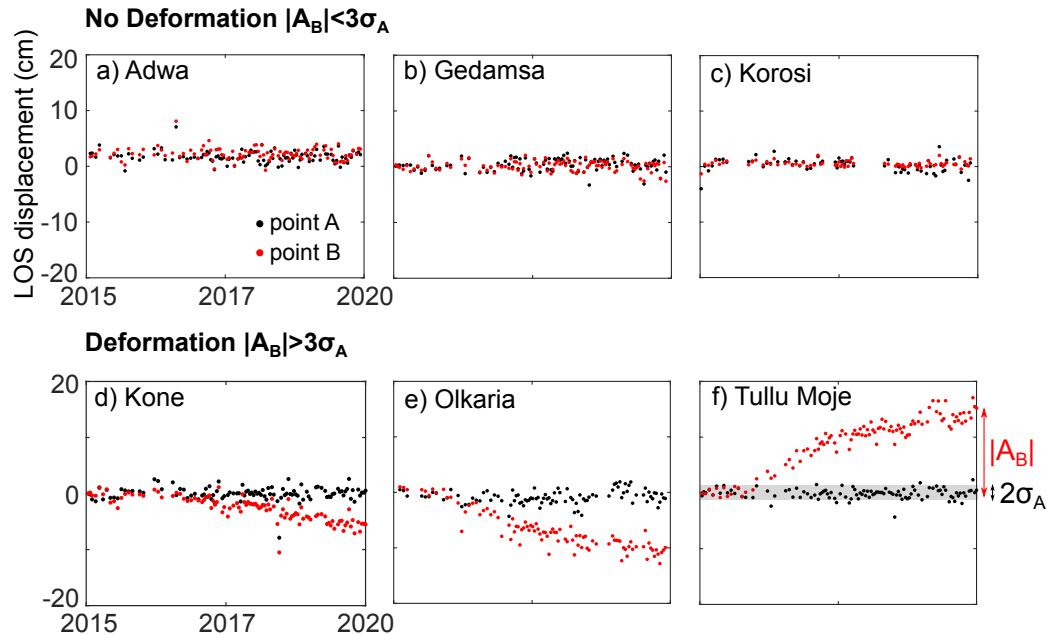


Figure S4. Examples of automated time series produced for a-c) three non-deformed volcanoes: Adwa, Gedamsa and Korosi and d-f) three deformed volcanoes: Kone, Olkaria and Tullu Moje. Black and red dots show the time series for the point A (baseline in non volcanic area) and the point B (signal in the volcanic area), respectively. The temporal standard deviation of the baseline (σ_A) characterises the level of noise whereas the magnitude of the cumulative displacement ($|A_B|$) characterises the amplitude of the signal.

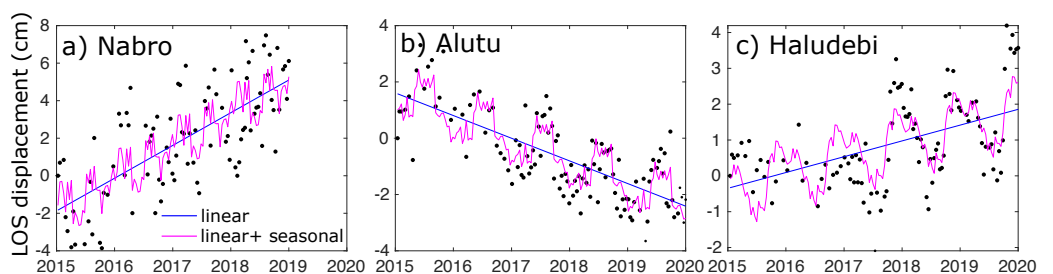


Figure S5. Seasonal signals superposed to linear trend observed in the volcanoes a) Nabro, b) Alutu and c) Haledebi.